Characterisation of heavily irradiated dielectrics for AC-coupled pixel detectors

S. Bharthuar[1,2], M. Golovleva [1,4], M. Bezak[1,4], E. Brücken[1,2], A. Gädda[1,6], A. Karadzhinova-Ferrer [1,5], N. Kramarenko [1,4], S. Kirschenmann [1,2], P. Luukka [1,4], K. Mizohata [2] J. Ott [1,3], and E. Tuominen [1,2]

[1]Helsinki Institute of Physics, Finland; [2]Department of Physics, University of Helsinki, Finland; [3]Aalto University, Finland; [4]Lappeenranta-Lahti University of Technology, Finland; [5]Ludong University, China; [6]Okmetic Oy, Finland

Email: shudhashil.bharthuar@cern.ch

23rd International Workshop on Radiation Imaging Detectors, 26–30 June 2022, Riva del Garda, Italy

Introduction

- The Phase-II upgrade of LHC to HL-LHC allows an increase in the operational luminosity value by a factor of 5-7. As a consequence of this, silicon detector layers within the inner tracker of the CMS experiment will be exposed to increased radiation doses up to 2.3×10^{16} n_{eq}/cm^2.
- Use of p-type Si with segmented n^+-implants allows electrons with higher mobility to be collected.

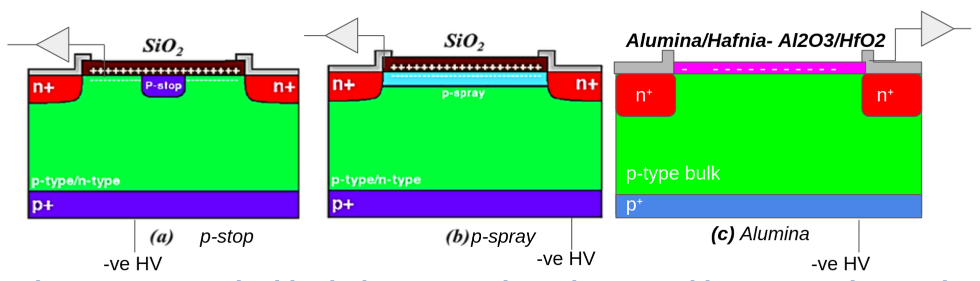

Figure 1 : Inter-pixel isolation strategies: a) p-stop, b) p-spray, c) negative oxide with high *k*-value.

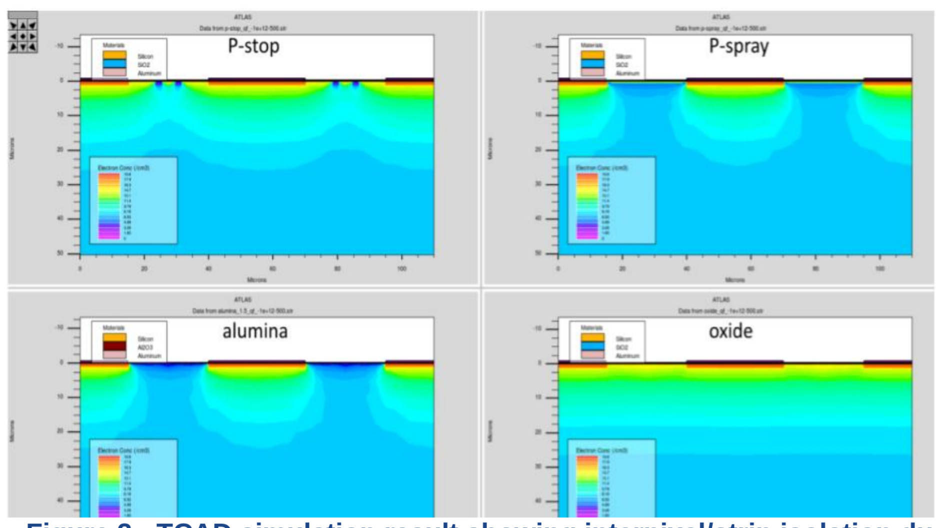

Figure 2 : TCAD simulation result showing interpixel/strip isolation due to p-stop/p-spray [top] and in case of a use of a negative oxide as insulating layer (such as alumina) [bottom-left].

- **Challenge:** electron accumulation near the interface of SiO_2 (positive oxide charge) insulating layer and p-bulk, leading to short circuit channel between n^+ implants.
- **Mitigation:** traditional ways include p-stop and p-spray that requires additional implantation and high temperature process steps.
- **Alternatively**, use of negative oxide like Al_2O_3 or HfO_2 - As high-k value permits higher oxide capacitance and high negative charge ($\sim 10^{-11}$-10^{-13} cm^{-2}).

Thin films of Al_2O_3 or HfO_2 are deposited using **Atomic Layer Deposition (ALD)** technique : require low temperatures, provides high uniformity of layers, very thin layers (tens of nm) with good accuracy [3, **?**].

Samples Measured

- Starting material: p-type MCz 6" Si, resistivity : 6-8 kΩcm, thickness: 320 µm. Fabricated at Micronova Nanofabrication Centre, in Finland.
- Main devices characterised for this study are:
  1) MOS capacitors and MOSFET
  2) Pad structure: PIN diodes
  3) AC coupled devices —–> design of PSI46dig sensor (52 × 80 pixel matrix), 150×100 µm pitch
- Comparison based on the characterisation of devices with : 1) Al_2O_3, 2) Al_2O_3 + HfO_2. HfO_2 2.7 times higher-k value than Al_2O_3
- The samples were irradiated with 10 MeV protons at the Accelerator Laboratory in University of Helsinki, Finland and gamma rays (Co-60 source) at RBI in Zagreb, Croatia.

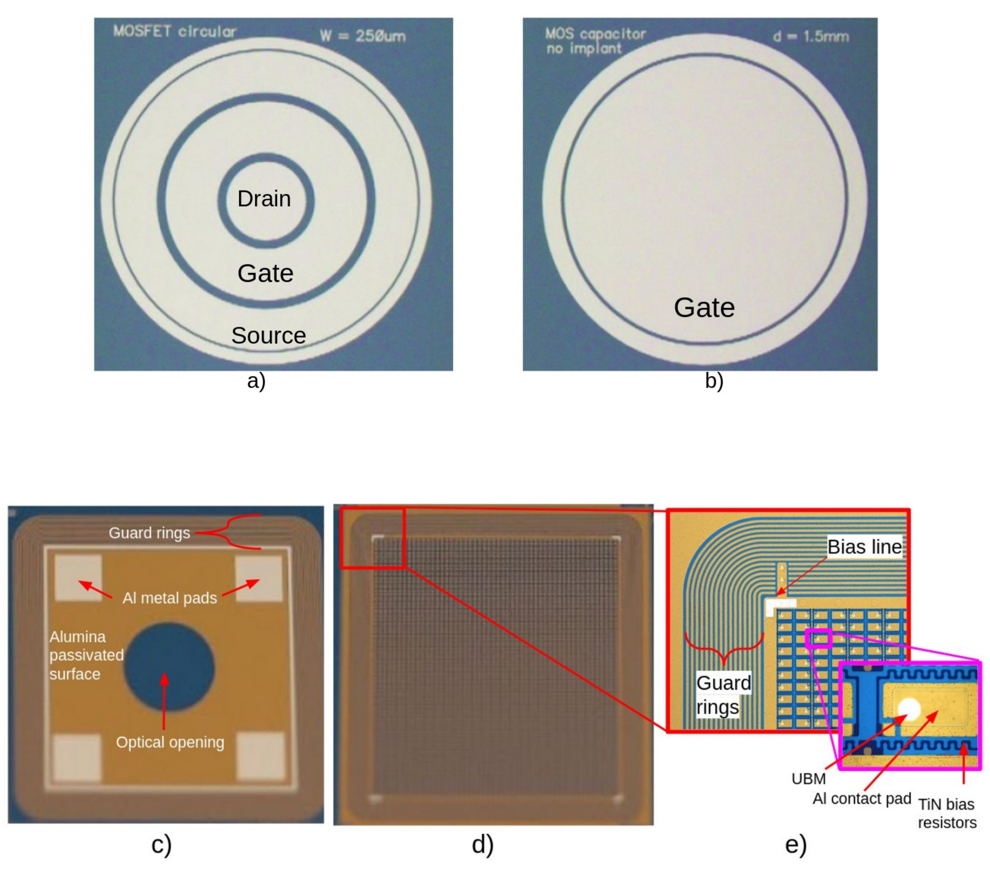

Figure 3 : Measured samples: a) MOSFET, b) MOS capacitor, c) Pad diode, d) AC-coupled pixel sensor with metal bias implants and e) showing zoomed and detailed structures within the pixel detector.

Electrical Characterisation

MOS capacitor

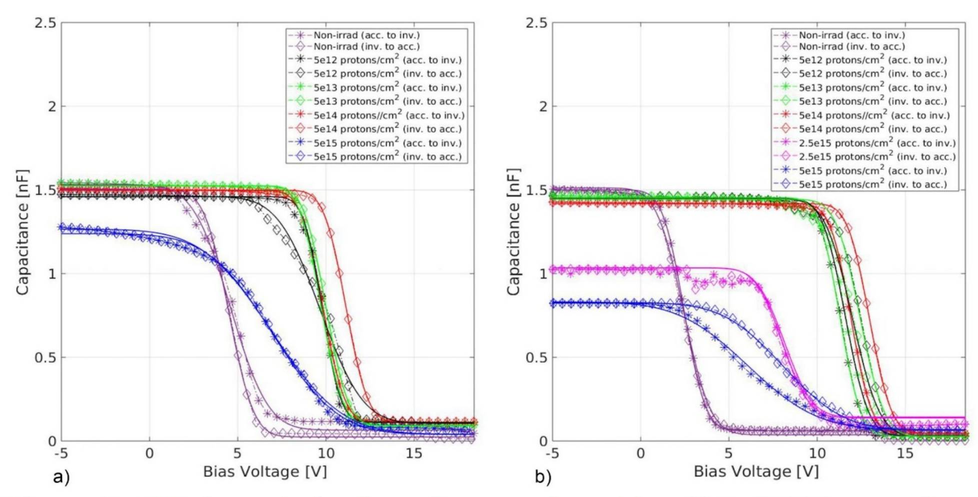

Figure 4 : CV characterisation of pre- and post-irradiated MOS capacitors.

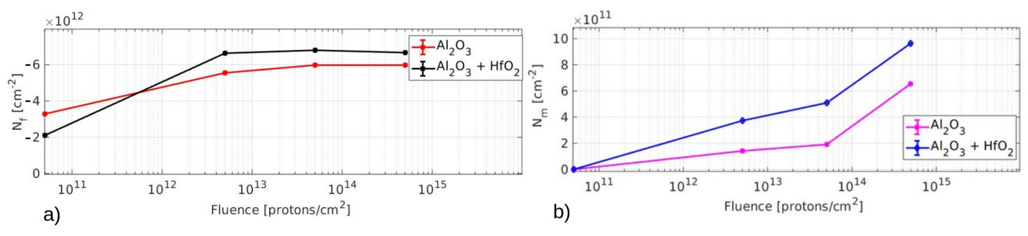

Figure 5 : Evolution of effective a) fixed charges and b) mobile charges in proton irradiated MOS capacitors with different insulating layers.

- Decrease in the fixed oxide charges (N_f) by a factor of $\sim$ 1.5 is observed for samples with HfO_2, as shown in Figure 5a —–> extracted from shift in flat-band voltage (V_{fb}) of MOS capacitors
- Hysteresis of CV curves in Figure 4, aids in analysing the concentration of mobile charges (N_m) which is a factor of $\sim$ 1.6 times higher in samples with Al_2O_3 + HfO_2 as dielectric layer.

Comparison of MOSFET Sensitivity

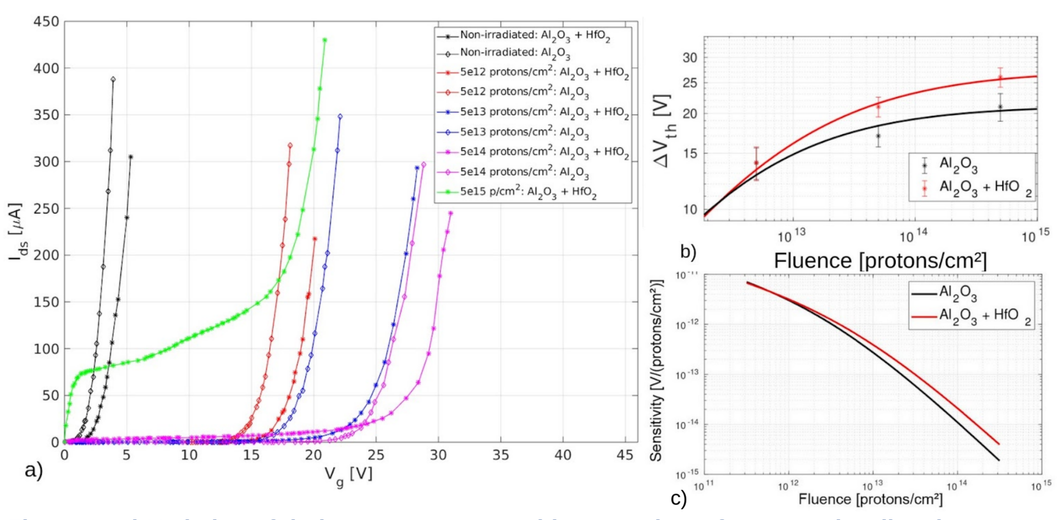

Figure 6 : a) Variation of drain-source current with gate voltage for proton irradiated MOSFETs, measured with a constant drain-to-source voltage of 1 V. b) Change in the shift and c) variation in the sensitivity with fluence for proton irradiated MOSFETs with different oxides.

- ΔV_{th} is positive for n-channel MOS transistors due to negative charge accumulation at the interface, forming the interface-traps.
- ΔV_{th} dependence on fluence is provided by the fitting equation (as shown in Figure 6b):

$$\Delta V_{th} = a + \frac{a}{1 + bD^c} \quad (1)$$

where, D is the proton fluence and (a, b, c) are three curve-fit parameters.

- Sensitivity, defined as the ratio of ΔV_{th} and fluence, as shown in Figure 6c, indicate samples with HfO_2 have higher sensitivity to irradiation, specifically at fluences above 10^{12} protons/cm^2.

AC-coupled pixel sensors

IV/CV measurements

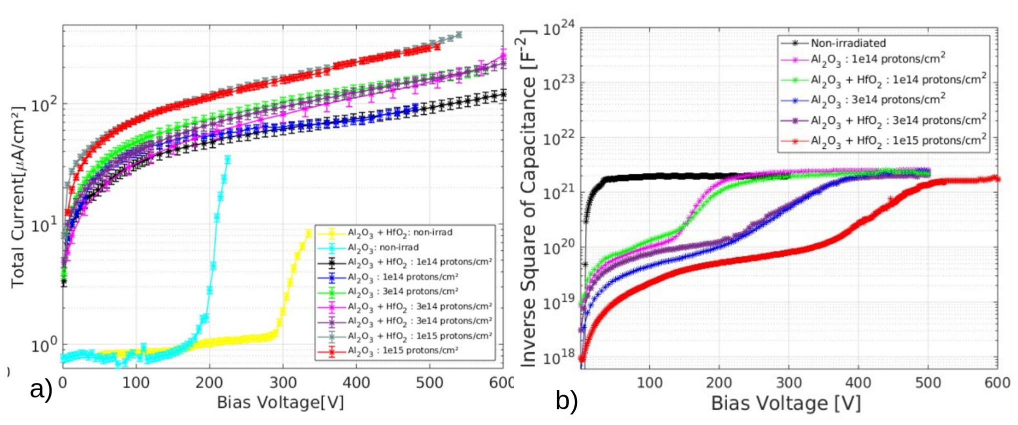

Figure 7 : a) Total leakage current of pre- and post-irradiated pixel sensors versus bias voltage for AC-coupled pixel sensors with different dielectric layers measured at -15ºC. b) Inverse square capacitance versus bias voltage curves for AC-coupled pixel sensors with combination of HfO_2 and Al_2O_3 used as the dielectric layer irradiated up to a fluence of 10^{15} protons/cm².

- AC-pixel senors with HfO_2 can sustain higher bias voltages as it provides better insulation than sensors with Al_2O_3 alone.

TCT measurements

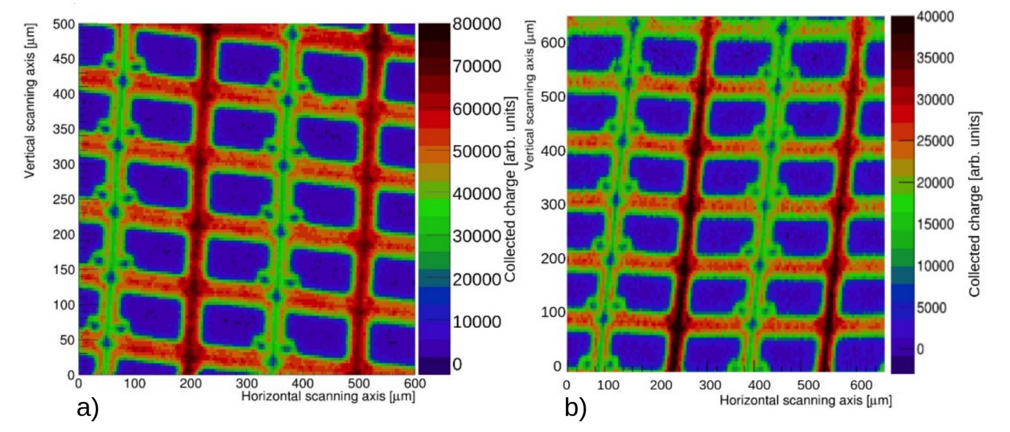

Figure 8 : Spatial homogeneity scans performed at a bias of 300 V with front illumination of IR-laser showing a scanned area of a) 500 × 600 µm² for 10^{14} protons/cm² and b) 620 × 650 µm² for 10^{15} protons/cm² irradiated AC-coupled pixel sensors with combination of HfO_2 and Al_2O_3 used as the dielectric layer.

- TCT characterisation of AC-coupled pixel sensors, shown in Figure 8, portray the spatial homogeneity across pixel scanned area —–> Maximum collected charge within the active region of the sensor is reduced by a factor of 2.25 (approx. 55%) at 10^{15} protons/cm^2.

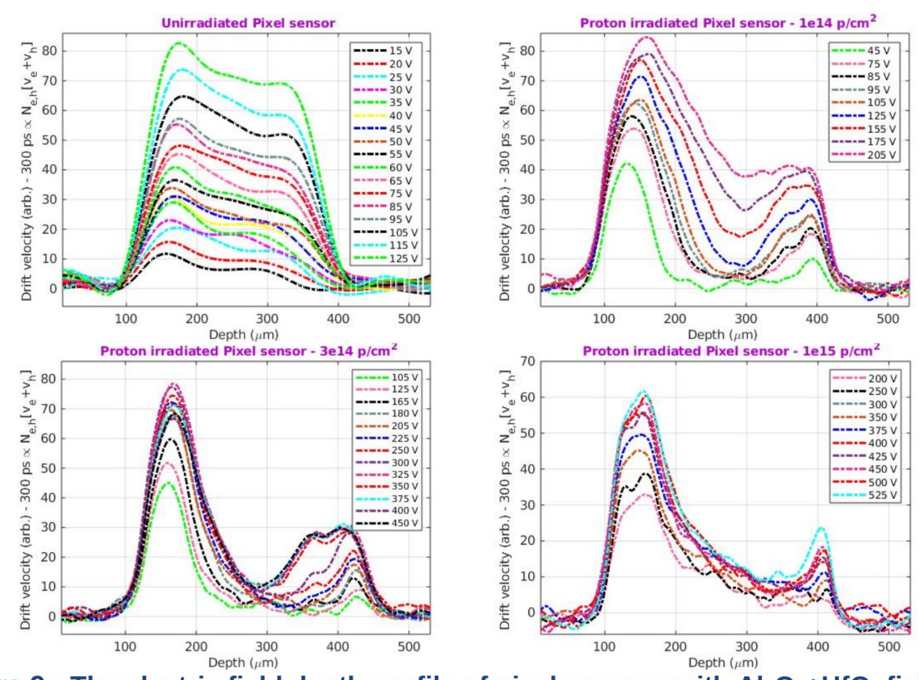

Figure 9 : The electric field depth-profile of pixel sensors with Al_2O_3+HfO_2 field insulation for various bias voltages: (top left to bottom right) non-irradiated; after fluence of 10^{14} p/cm²; after fluence of 3 ×10^{14} p/cm²; after fluence of 10^{15} p/cm².

- Electric field is numerically determined from the drift velocity profiles using the prompt method in edge-TCT (e-TCT) measurements, shown in Figure 9a.
- Characteristic double-peak effect in the electric field prominent for sensors irradiated above 10^{14} protons/cm^2. Less pronounced for higher bias voltages as the MCz-silicon wafers possess a high concentration of oxygen of a magnitude of $\sim 10^{17}$ cm^{-3} responsible for the suppression of deep-level trap formation by decreasing the mid-gap defect concentrations [2].

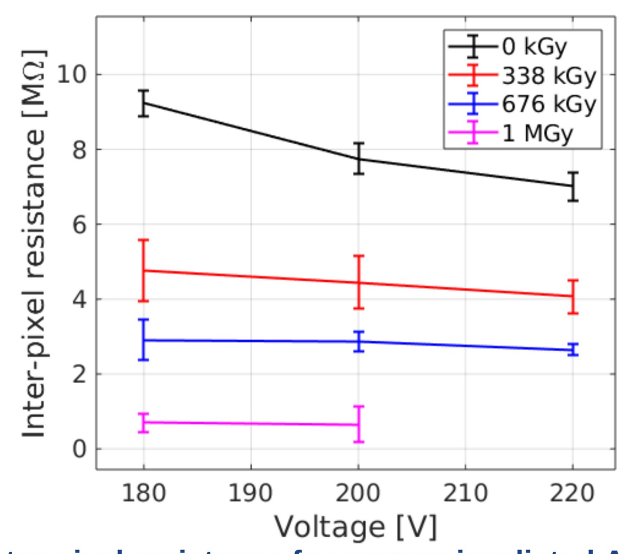

Figure 10 : Inter-pixel resistance for gamma irradiated AC-pixel sensors.

- The inter-pixel resistance measured between the pixels decreases by a factor of $\sim$ 5.4 on gamma irradiation up to doses of 1 MGy, as shown in Figure 10.

Conclusion

- Negative oxide charge during irradiation is an essential prerequisite of radiation hardness resiliency of $n^+/p^-/p^+$ (n on p) detectors widely intended to be used in future high-luminosity experiments.
- MOS devices with HfO_2 + Al_2O_3 posses higher sensitivity to irradiation, when irradiated to high fluences, in comparison with Al_2O_3 alone as the oxide layer.
- Studies based on e-TCT measurements show promising electric field profiles. However, double-junction effect as a consequence of deep-level traps in the band-gap of silicon was identified in proton irradiated samples.

References

[1] S. Bharthuar, et al. Characterization of heavily irradiated dielectrics for pixel sensors coupling insulator applications. *Frontiers in Materials*, 8, 2022.

[2] V. Eremin, et al. The origin of double peak electric field distribution in heavily irradiated silicon detectors. *Nuclear Instruments and Methods in Physics Research A*, 476(3):556–564.

[3] J. Ott, et al. Processing of AC-coupled n-in-p pixel detectors on MCz silicon using atomic layer deposited aluminium oxide. *Nuclear Instruments and Methods in Physics Research A*, 958:162547.